



Synthesis, Structural Properties and Water Oxidation Activity of Iron (III) Complexes with Salophen Ligands

Zohreh Shaghghi^{1*}, Habibeh Tajdar², Mehri Aligholivand³

^{1,2,3} Coordination Chemistry Research Laboratory, Department of Chemistry, Faculty of Science, Azarbaijan Shahid Madani University, 5375171379, Tabriz, Iran

E-mail: shaghghi@azaruniv.ac.ir, zsh024@gmail.com

Received: 2024-01-25, Accepted: 2024-05-03

Abstract

In this work, Fe^{III} salophen complexes **1-3** were prepared from the reaction of H₂L¹⁻³ (H₂L¹=N,N'-bis(salicylidene)-4-chloro-1,2-phenylenediamine, H₂L²=N,N'-bis(salicylidene)-4-bromo-1,2-phenylenediamine, and H₂L³=N,N'-bis(salicylene)-4-nitro-1,2-phenylenediamine) with FeCl₃.6H₂O. The structure of the complexes was investigated by spectroscopic techniques, molar conductivity measurements and elemental analysis. In addition, water oxidation activity of complexes was investigated by different electrochemical methods in alkaline solution. The results showed that the compounds reveal high performance for water oxidation in terms of overpotential and Tafel slope values. Fe^{III} complex **3** displayed the best activity for the reaction with low overpotential of 485 mV at a j of 10 mA cm⁻² and a suitable Tafel slope of 216 mV dec⁻¹ among other complexes. This is due to larger electrochemically active surface area of **3**, which leads to more active catalytic sites and improved water oxidation activity. Finally, the chronoamperometry test revealed that **3** is a stable and durable electrocatalyst for water oxidation.

Keywords: Iron(III) complexes, Salophen-type ligands, Electrocatalyst, Electrochemistry, Water oxidation

Introduction

Synthesis and design of iron(III) complexes with N_2O_2 ligands has always been an interesting field of research [1-6]. These complexes can be used as synthetic models for iron-containing enzymes [7-9]. They also can be used as catalysts for various asymmetric reactions [10, 11]. In addition, many non-heme iron metalloproteins having several active sites with mononuclear iron centers are biologically important [12, 13]. Iron can take various oxidation states from -2 to +6, but the most common iron oxidation numbers are +2 and +3. The redox potential of Fe^{3+}/Fe^{2+} couple depends on the type of ligands around it and, this facilitates the catalytic role of iron in biological systems [14]. For these reasons, the coordination chemistry of Fe complexes has always been of interest to researchers. For example, Basak et al. [15] reported two mononuclear iron(III) complexes containing *N,N'*-bis(3-methoxysalicylidene)diethylenetriamine, *N,N'*-bis(3-ethoxysalicylidene)diethylenetriamine and azide ligands. They also studied the band gap and conductivity of the complexes. The results showed that the complex with methoxy substitute is a better candidate for electronic device applications. Boca and coworkers investigated magnetic properties of some pentacoordinate Fe^{III} complexes with bidentate Schiff-base N and O donor ligands [16]. They found that a distant ethoxy group to the methoxy residing at the phenyl ring of ligand influences the relaxation characteristics. Sharghi and coworkers applied the Fe^{III} salen complex as a catalyst for the synthesis of benzoaxazol derivatives from catechols, ammonium

acetate and aldehydes for the first time [17]. Sonmez et al. [18] prepared some complexes with polydentate Schiff-base ligands containing phenoxy groups with Ru^{III} , Cr^{III} and Fe^{III} . Their findings that the Fe^{III} complex reveals very efficient catalytic activity in the green synthesis of vitamin K_3 from 2-methylnaphthalene. Moreover, another important application of iron(III) complexes is their valuable catalytic role in the water splitting reaction, which have received special attention in recent years. Water splitting, which leads to the production of oxygen and hydrogen, is one of the most promising ways to storage energy [19-23]. For example, some iron (III) complexes with nitrogen and oxygen donor ligands that have been used as catalysts for the oxidation of water are: *cis*- $[Fe(cyclam)Cl_2]Cl$ (cyclam= 1,4,8,11-tetraazacyclotetradecane) [24], non-heme Fe^{III} complexes [25, 26], $Fe(salen)$ -MOF composite (salen= *N,N'*-bis(salicylidene)ethylenediamine, MOF=metal-organometallic framework) [27], Fe -TAML (TAML=tetraamido macrocyclic ligand) [28], six coordinate Fe^{III} aqua complex, $[Fe^{III}(dpaq)(H_2O)]^{2+}$ (dpaq= 2-[bis(pyridine-2-ylmethyl)]amino-*N*-quinolin-8-yl-acetamido) [29], pentanuclear iron complexes, $[Fe_4^{II}Fe^{III}(\mu_3O)(Me-bpp)_6](PF_6)_3$, $[Fe_5-Me](PF_6)_3$, $[Fe_4^{II}Fe^{III}(\mu_3O)(Br-bpp)_6](PF_6)_3$, $[Fe_5-Br](PF_6)_3$ (4-substituted-3,5-bis(pyridyl)pyrazole) [30], $[Fe_4^{II}Fe^{III}(\mu-L)_6(\mu-O)] \cdot (BF_4)_3(H_2O)_n$ (LH: 2,2'-(1H-pyrazole-3,5-diyl)dipyridine) [31] and so on.

Among the Schiff-base complexes of iron with N and O donor ligands, Fe -salophen complexes have attracted a lot of attention

due to their stability, ease of preparation and excellent electrochemical behavior [32-37]. Salophens are tetradentate N_2O_2 Schiff base ligands which are produced from the condensation reaction of 1,2-phenylenediamine derivatives with two equivalents of salicylaldehyde derivatives. Although there are many reports of mononuclear and binuclear complexes of iron containing salophen type ligands, synthesis and study of properties of Fe-salophen complexes and their application in catalytic processes are still of interest to researchers.

The aim of the present study is to synthesis and investigate of important structural properties and water oxidation activity of a number of iron(III) complexes with salophen ligands containing different electron-withdrawing substituents. Thus, in our continuing research on the coordination chemistry of salophen type ligands [19, 20, 32, 37, 38], in this work we report experimental studies and water oxidation activity of iron(III)-salophen complexes with different electron-withdrawing substituents on the central phenyl ring of ligands. The results show that these compounds can catalyze the water oxidation reaction as stable and molecular electrocatalysts, and complex **3** shows the highest activity in terms of overpotential and Tafel slope values compared to complexes **1** and **2**.

Experimental

Materials and Instruments

N_2O_2 Schiff-base ligands, H_2L^{1-3} , N,N' -bis(salicylidene)-4-chloro-1,2-

phenyldiamine, N,N' -bis(salicylidene)-4-bromo-1,2-phenyldiamine, and N,N' -bis(salicylidene)-4-nitro-1,2-phenyldiamine were prepared according to the literature [38]. FT-IR spectra of compounds were obtained by a FT-IR Spectrometer Bruker Tensor 27 with using KBr pellet. Electronic absorption spectra were recorded with T 60 UV/Vis Spectrometer PG Instruments Ltd. The elemental analyses of the complexes were obtained from an Elementar elx III. Cyclic voltammograms of complexes were recorded using an Autolab PGSTAT204.

General method for synthesis of Fe^{III} complexes

An ethanol solution (20 mL) of $FeCl_3 \cdot 6H_2O$ (0.189 g, 0.700 mmol) was slowly added to the solution of Ligands, H_2L^{1-3} (0.700 mmol) in dichloromethane (15 mL) at room temperature. Immediately, the color solution was changed and a precipitate was formed. The reaction was continued for 4 h (the reaction end was controlled by thin layer chromatography). Finally, the mixture reaction was filtered, the residue recrystallized by ethanol-dichloromethane solvents and dried.

Fe^{III} complex with H_2L^1 (**1**)

A dark brown powder was achieved (0.230 g, Yield: 74.91%). IR (KBr, cm^{-1}) 3446 (br), 1601 (s), 1573 (s), 1531(s), 1461 (m), 1439 (m), 1373 (s), 1319 (s), 1194 (w), 1146 (w), 1093 (m), 903 (m), 857 (m), 815 (s), 760 (s), 603 (w), 547 (w), 497 (w), 475 (w), 432 (w). Elem. Anal. Calc. for $C_{20}H_{13}FeO_2N_2Cl_2$ ($M_w = 439.74$ g mol^{-1}): C, 54.58; H, 2.96; N, 6.36%. Found: C, 55.09; H, 3.23; N%, 6.69. UV-vis in DMSO (λ_{max} [nm] with ϵ [$M^{-1}cm^{-1}$]

¹): 263 (9800), 303 (14700), 386 (8400), 442 (4200).

Fe^{III} complex with H₂L² (2)

A dark brown powder was achieved (0.285 g, Yield: 82.84 %). IR (KBr, cm⁻¹): 3449 (br), 1601 (s), 1571 (s), 1533 (s), 1487 (m), 1461 (m), 1437 (m), 1372 (s), 1311 (s), 1194 (w), 1149, 926, 858, 761 (s), 602 (w), 545 (m), 495 (w), 475 (w). Elem. Anal. Calc. for C₂₀H₁₄FeO_{2.5}N₂ClBr (M_w= 492.75 g mol⁻¹): C, 48.70; H, 2.84; N, 5.68%. Found: C, 49.31; H, 2.96; N%, 5.69. UV-vis in DMSO (λ_{max} [nm] with ε [M⁻¹cm⁻¹]): 266 (23333), 304 (33333), 385 (20066), 440 (4200).

Fe^{III} complex with H₂L³ (3)

A dark brown powder was achieved (0.250 g, Yield: 73.52 %). IR (KBr, cm⁻¹) 3422 (br), 1604 (s), 1573 (s), 1522 (s), 1462 (m), 1437 (m), 1377 (s), 1343 (s), 1310 (s), 1196 (w), 1150 (w), 1085 (m), 914 (m), 860 (m), 803 (m), 766 (s), 603 (w), 552 (w), 482 (w), 420 (w). Elem. Anal. Calc. for C₂₀H₁₇FeO₆N₃Cl (M_w=486.25 g mol⁻¹): C, 49.35; H, 3.49; N, 8.64%. Found: C, 50.10; H, 3.55; N%, 8.65. UV-vis in DMSO (λ_{max} [nm] with ε [M⁻¹cm⁻¹]): 271 (9033), 311(17433), 396 (10800), 452 (6433).

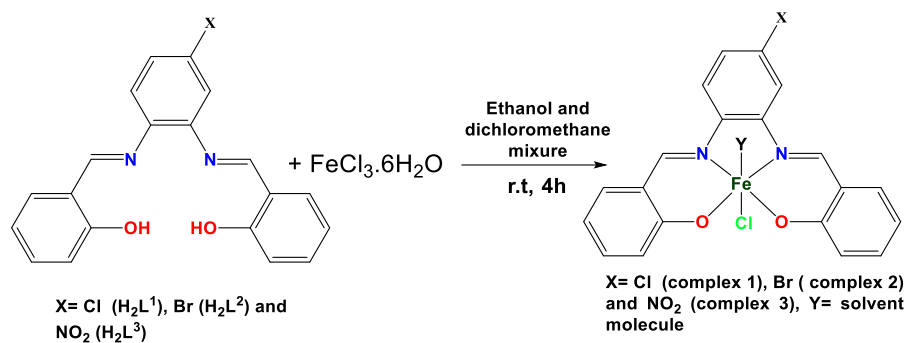
Fabrication of modified electrodes

To produce modified electrodes with Fe complexes **1-3**, graphite, paraffin, and Fe complexes **1-3** with a mass ratio of 80: 5: 15

were thoroughly mixed and homogenized for at least 2 hours. Then the obtained pastes were placed in copper wires with a radius of 1.1 mm. The surface of electrodes was washed several times with diluted water and completely smoothed before use. To prepare the unmodified electrode, paraffin and graphite were mixed with a mass ratio of 20:80 and after homogenization, they were placed in a copper wire. All electrochemical experiments were carried out in a three-electrode system containing Ag/AgCl, Pt wire, and unmodified or modified carbon past electrodes as reference, counter, and working electrodes in the presence of 25 mL of borate solution (0.5 M, pH=11).

Results and discussions

Fe^{III} complexes **1-3** were prepared from the reaction of FeCl₃·6H₂O with salophen type ligands, H₂L¹-H₂L³, in the mixture of dichloromethane-ethanol solutions at room temperature for 4 h (Scheme 1). The complexes were studied by FT-IR and UV-vis spectroscopy, molar conductivity measurements, and elemental analysis. In addition, electrochemical properties and water oxidation activity of the complexes were investigated.



Scheme 1: The synthetic route of the Fe^{III} salophen complexes **1-3**

Structural characterizations

Some important FT-IR spectroscopy data of the complexes are given in Table 1. In the spectra of the complexes, the stretching vibration of $-\text{C}=\text{N}-$ of imine groups appears in $1600\text{-}1604 \text{ cm}^{-1}$ wavenumbers which shifts to the lower frequency compared to the free ligands [37]. This may be due to the bounding of the nitrogen atoms of imine groups of Schiff-base ligands to the Fe^{III} ion centers [32, 39]. The appearance of the broad peak at $3422\text{-}3449 \text{ cm}^{-1}$ region can be assigned to the stretching vibration of coordinated water molecules. In addition, the stretching vibrations of Fe-O and Fe-N are observed as weak peaks in the range of $420\text{-}552 \text{ cm}^{-1}$ [40]. UV-vis spectra of iron(III) complexes **1-3** are shown in Figure 1. In the UV-vis spectra of the complexes,

the absorption bands observed at around $263\text{-}339 \text{ nm}$ are attributed to the intra-ligand $\pi \rightarrow \pi^*$ and $n \rightarrow \pi^*$ transitions [41]. Changes in the intensity and position of $n \rightarrow \pi^*$ transition in the spectra of the complexes compared to the free ligands confirm the coordination of nitrogen atoms of imine groups to the Fe^{III} ion centers [32]. The broad absorption bands around $380\text{-}394 \text{ nm}$ and shoulders at $441\text{-}450 \text{ nm}$ are attributed to the charge transfer from the salophen ligand to the Fe^{III} ion center [42-44]. Also, the values of molar conductivity of Fe^{III} complexes **1-3** (10^{-3} M in DMSO) are 0.045 , 0.049 and $0.047 \text{ cm}^2 \Omega^{-1} \text{ mol}^{-1}$ respectively, which indicate their non-electrolyte nature. This can be due to the deprotonation of salophen ligands when binding to the metal ion center [20, 22, 32, 37].

Table 1: FT-IR data for Fe^{III} complexes **1-3**

Compound	$\nu (-\text{C}=\text{N}-), (\text{cm}^{-1})$	$\nu (\text{H}_2\text{O}), (\text{cm}^{-1})$	$\nu (\text{NO}_2), (\text{cm}^{-1})$	$\nu (\text{C-Cl}), (\text{cm}^{-1})$	$\nu (\text{C-Br}), (\text{cm}^{-1})$	$\nu (\text{Fe-O}), (\text{Fe-N}), (\text{cm}^{-1})$
1	1601	3446	-	857	-	432-547
2	1601	3449	-	-	761	475-545
3	1604	3422	1343	-	-	420-552

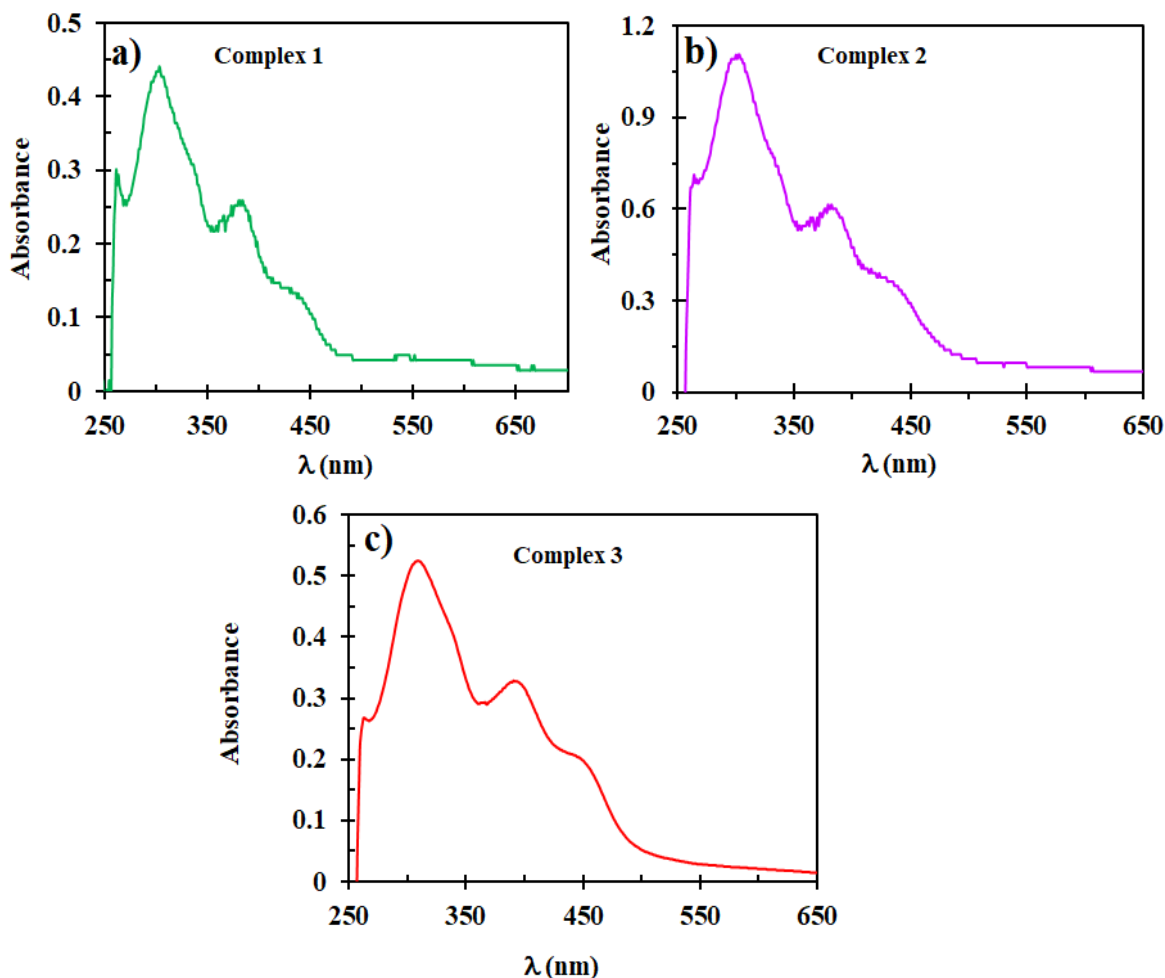


Figure 1: UV-Vis spectra of Fe^{III} complexes **1-3** in DMSO (3×10^{-5} M).

Electrochemical studies

Figure 2 shows cyclic voltammograms of Fe^{III} complexes **1-3** in DMSO solution containing 0.1 M LiClO₄ as a supporting electrode at room temperature and the scan rate of 50 mV s⁻¹. Fe complexes **1-3** display one electron reversible oxidation and reduction process. In the voltammograms of the complexes, the anodic peak at the range of -1.28 to -1.32 are assigned to the oxidation of Fe(II) to Fe(III), and the

cathodic peak at the range of -1.42 to -1.46 V are attributed to the reduction of Fe(III) to Fe(II) [32]. It should be noted that the anodic peak observed at about -0.65 V and the cathodic peak observed at about -0.75 V are related to the reversible oxidation and reduction of their respective ligands [32, 37]. Finally, the anodic wave observed at the range of 0.52- 0.64 V is related to the irreversible oxidation of the salophen ligands [32, 37]. The electrochemical data are summarized in Table 2.

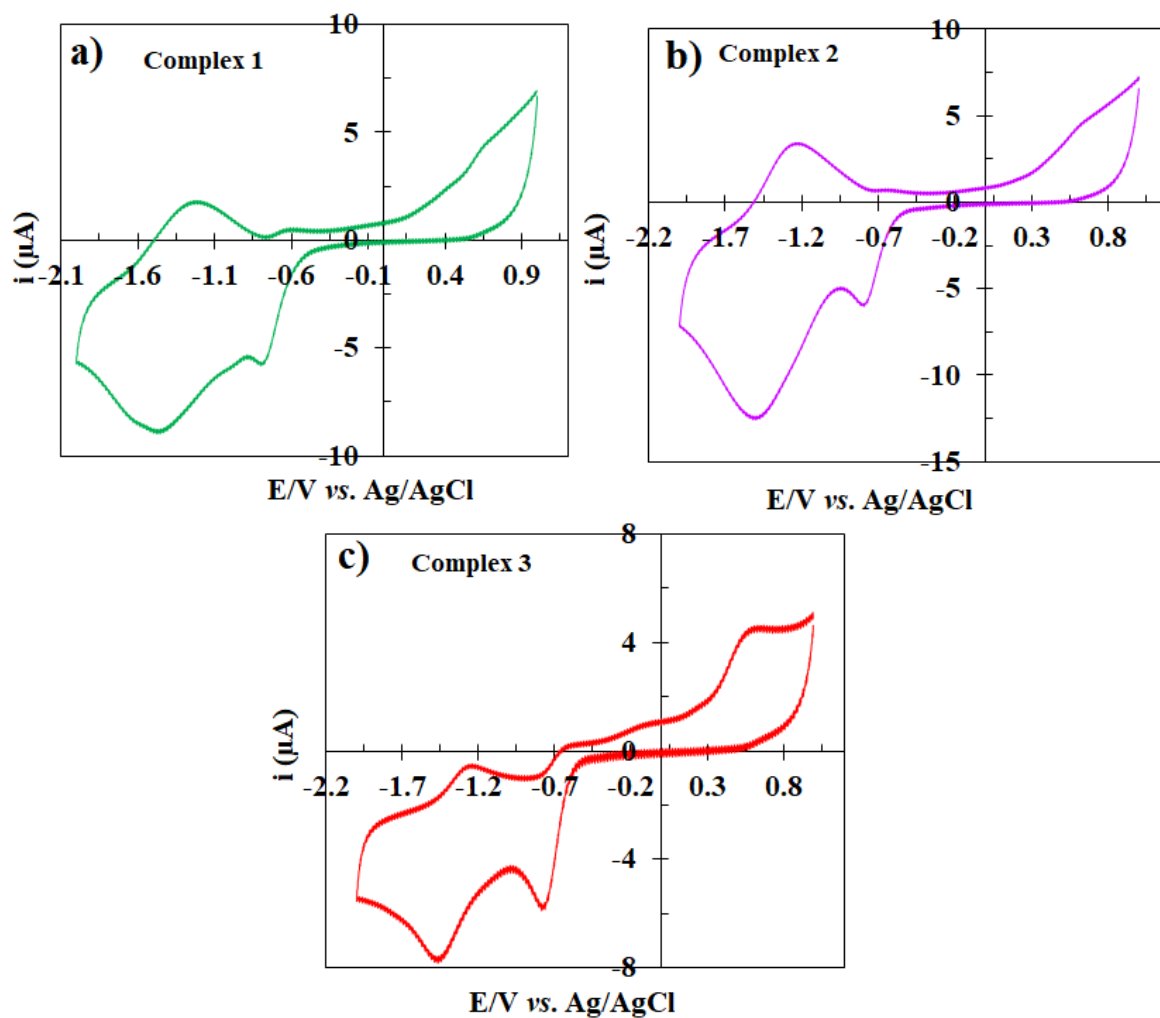


Figure 2: Cyclic voltammograms of Fe^{III} complexes **1-3** in DMSO solution containing 0.1 M LiClO₄ as a supporting electrolyte at the sweep rate of 50 mV s⁻¹.

Table 2: Electrochemical data for Fe complexes **1-3** in DMSO solution (10⁻³ M)

Compound	E _{pa} (V)	E _{pc} (V)	E _{1/2} /V (ΔE _p (mV))
Complex 1	-1.28	-1.42	-1.35 (140)
	-0.650	-0.750	-0.70 (100)
	0.640		
Complex 2	-1.30	-1.46	-1.38 (160)
	-0.68	-0.76	-0.720 (80)
	0.62		
Complex 3	-1.32	-1.43	-1.375 (110)
	-0.650	-0.74	-0.695 (90)
	0.52		

Water oxidation activity

In this section, water oxidation activity of Fe complexes **1-3** was investigated by Linear sweep voltammetry (LSV), cyclic voltammetry (CV), and chronoamperometry (CA) techniques in borate solution (0.5 M, pH=11). Figure 3a shows the LSV plots of the carbon paste electrode in the absence and presence of Fe salophen complexes **1-3** at the scan rate of 50 mV s^{-1} . As considered, bare carbon paste electrode (electrode without electrocatalysts) does not show any significant activity towards the water oxidation reaction. But, when any of the complexes are added to the carbon paste electrode, the water oxidation performance increases considerably. The onset potential for the reaction in the presence of the bare carbon paste electrode is greater than 1.5 V vs. Ag/AgCl at a current density of 10 mA cm^{-2} , while this value decreases to 0.98, 1.03 and 0.84 V in the presence of Fe complexes **1-3**, respectively under the same conditions. As can be seen, complex **3** needs the lowest onset potential to generate a current density of 10 mA cm^{-2} for water oxidation among all tested compounds. Fe complex **3** needs a relatively low overpotential of 485 mV, while complexes **1** and **2** needs an overpotential value of 625 and 675 mV under the same conditions. The overpotential values at j of 5, 10, and 20 mA cm^{-2} for all complexes are given in Figure 3b, which indicates the higher activity of complex **3** compared to complexes **1** and **2**. Cyclic voltammograms of carbon paste electrodes in the presence of electrocatalysts are shown in Figure 3c, which reveals that

complex **3** has the best activity for water oxidation. Furthermore, all voltammograms shows the $\text{Fe}^{\text{III}}/\text{Fe}^{\text{II}}$ redox couple [45], which indicates that the metal ion centers of the complexes participate in the reaction as active catalytic sites. To investigate the kinetics of the reaction in the presence of electrocatalysts, Tafel plots were obtained by plotting the potential versus the logarithm of the current density (Figure 3d). The slope value of these linear plots (Tafel slopes) is used to check the kinetics of the reaction, and a low Tafel slope indicate desirable kinetics. As shown in Figure 3d, Fe complex **3** has lower Tafel slope (216 mV dec^{-1}) than complexes **1** and **2** (227 and 313 mV dec^{-1}), and the kinetics of the oxidation of water in the presence of this complex is better. The better performance of complex **3** was proven by calculating the electrochemically active surface area (ECSA). ECSA is obtained from the equation: C_{dl}/C_s (C_{dl} = double layer capacitance and C_s =the specific capacitance of the electrode). C_{dl} is obtained from CVs performed at different scan rates and a plot of $\Delta j/2$ ($\Delta j=j_a-j_c$) versus scan rates in a non-faradaic region (Figure 4a-d). C_{dl} has a direct relationship with ECSA, and a large C_{dl} value indicates a large ECSA. Also, the higher ECSA, the number of active catalytic sites increases, and as a result, the electrocatalytic activity of the compound improves. As shown in Figure 4d, the Fe complex **3** has the largest C_{dl} value (5.21 mF cm^{-2}) compared to the other tested complexes (2.24 and 1.04 mF cm^{-2} for complexes **1** and **2**, respectively). Therefore, compound **3** has more active catalytic sites

and shows higher electrocatalytic activity

for water oxidation.

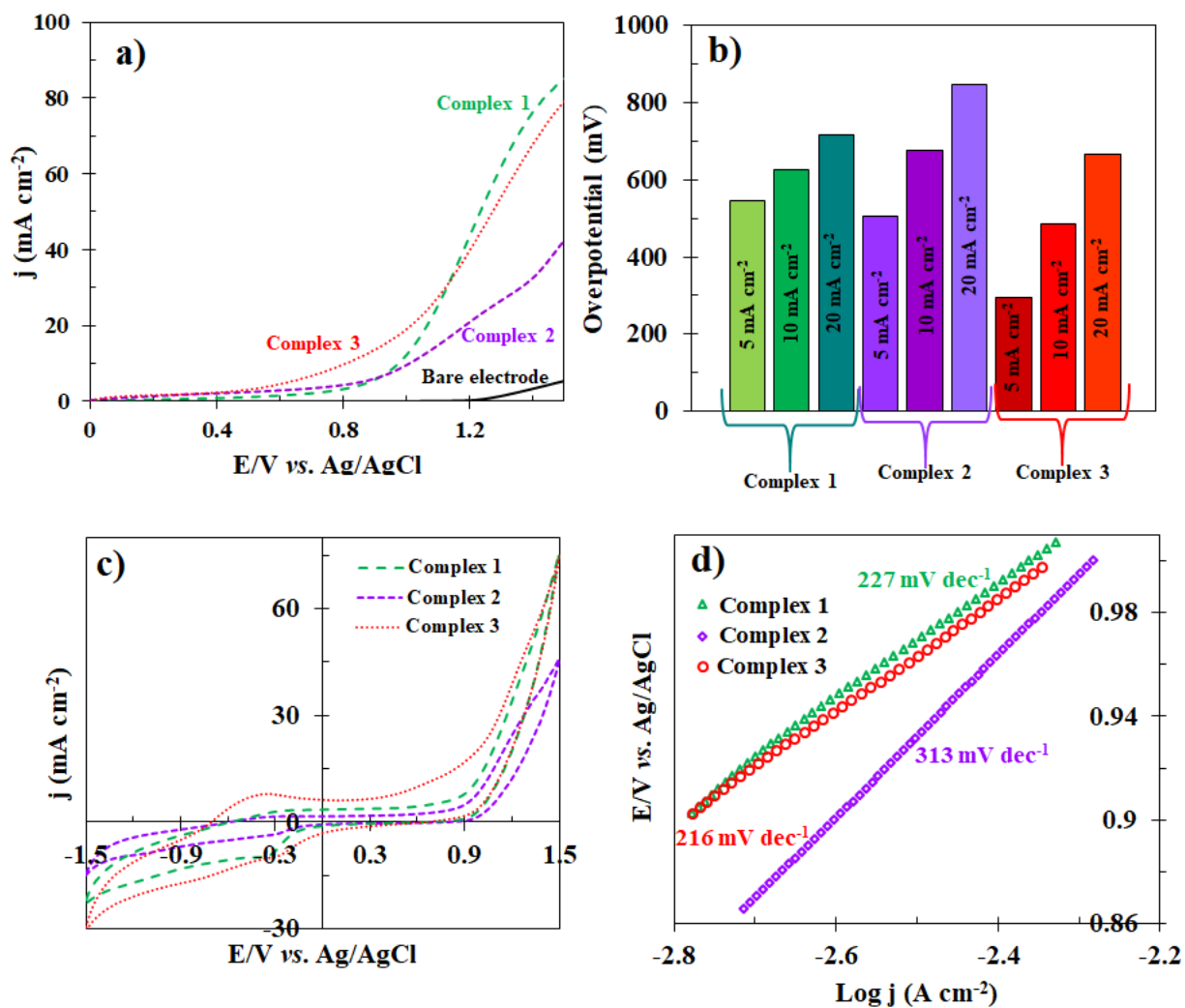


Figure 3: The LSV curves of carbon paste electrode in the absence and presence of Fe complexes 1-3 in a borate buffer solution (pH=11, 0.5 M) at a scan rate of 50 mV s^{-1} (a), the needed overpotential values at j of 5, 10, and 20 mA cm^{-2} for water oxidation in the presence of electrocatalysts (b), CVs of modified electrodes with Fe complexes 1-3 in a borate buffer solution (pH=11, 0.5 M) at a scan rate of 50 mV s^{-1} (c), and Tafel curves; obtained from CVs at a low scan speed of 5 mV s^{-1} (d).

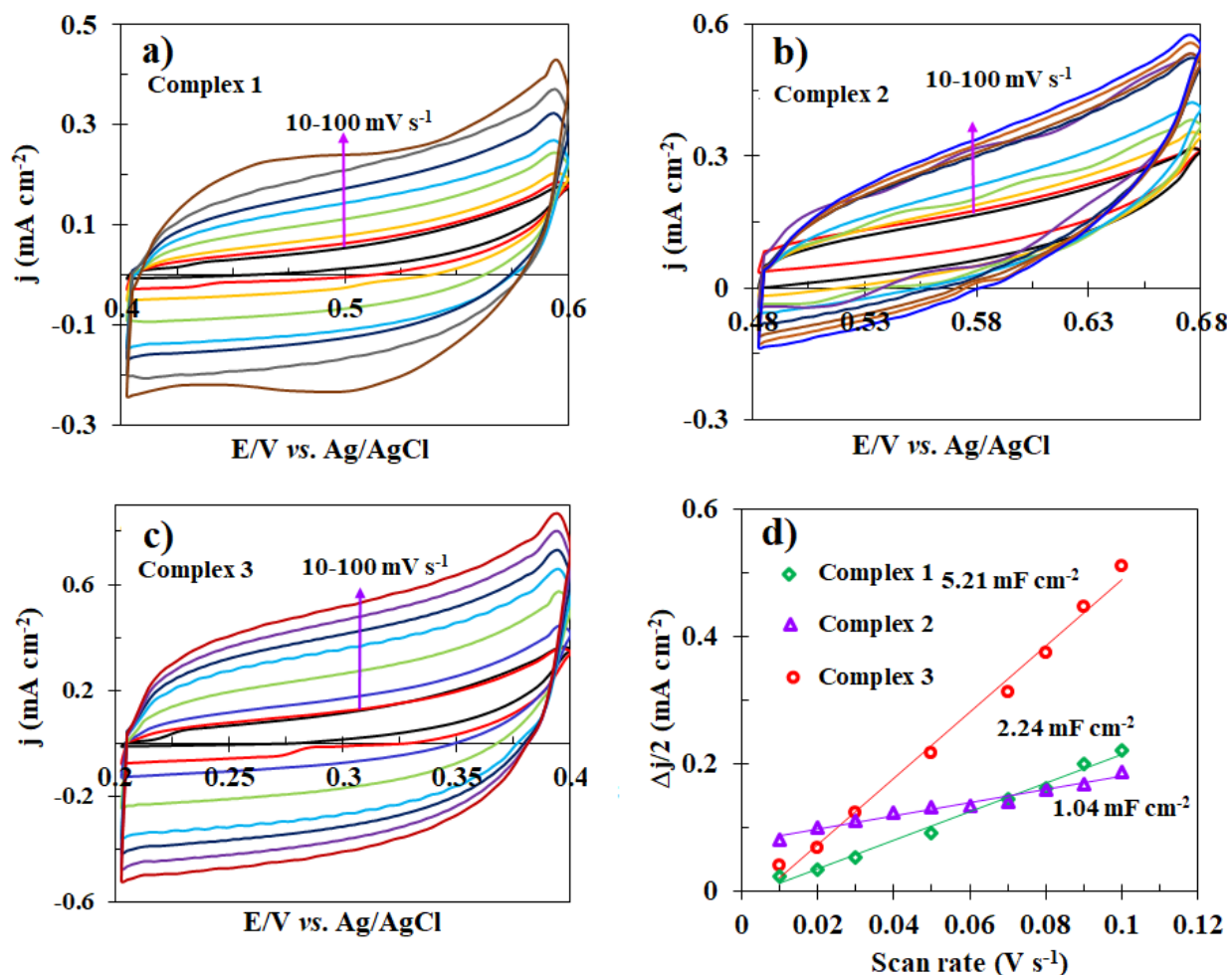


Figure 4: CVs of carbon paste electrodes modified by the Fe complexes **1-3** at different scan rates of 10-100 mV s⁻¹ in a non-faradaic region (a-c) and C_{dl} curves (d).

For further investigations, continuous CVs were performed in the presence of electrocatalyst (see Figure 5). As observed, for complexes **2** and **3**, the vertex current does not change much during successive 80 cycles, while for complex **1**, the peak current density increases during the first 20 cycles and then remains almost constant. In addition, the anodic and cathodic peaks related to the oxidation and reduction of the metal ion centers in the complex structure become more intense with the increase in the number of cycles, which indicates that

with the progress of the reaction, the number of Fe^{III} ions participating in the reaction as catalytic active sites increases [45]. No color change, no solid film formation on the electrode surface and no further change in the catalytic current density especially in the case of complex **3** are evidences that these complexes probably act as molecular electrocatalysts and their structure during the water oxidation reaction does not change [19]. Since, the Fe complex **3** had the best performance for water oxidation compared to the other complexes, the stability and

durability of this complex was investigated by the chronoamperometry technique at a constant potential of 0.8 V for 6 hours. The results are shown in Figure 6. As seen, a

stable current density about 2 mA cm⁻² is obtained during almost 6 h, which indicated the high stability of the complex during the reaction.

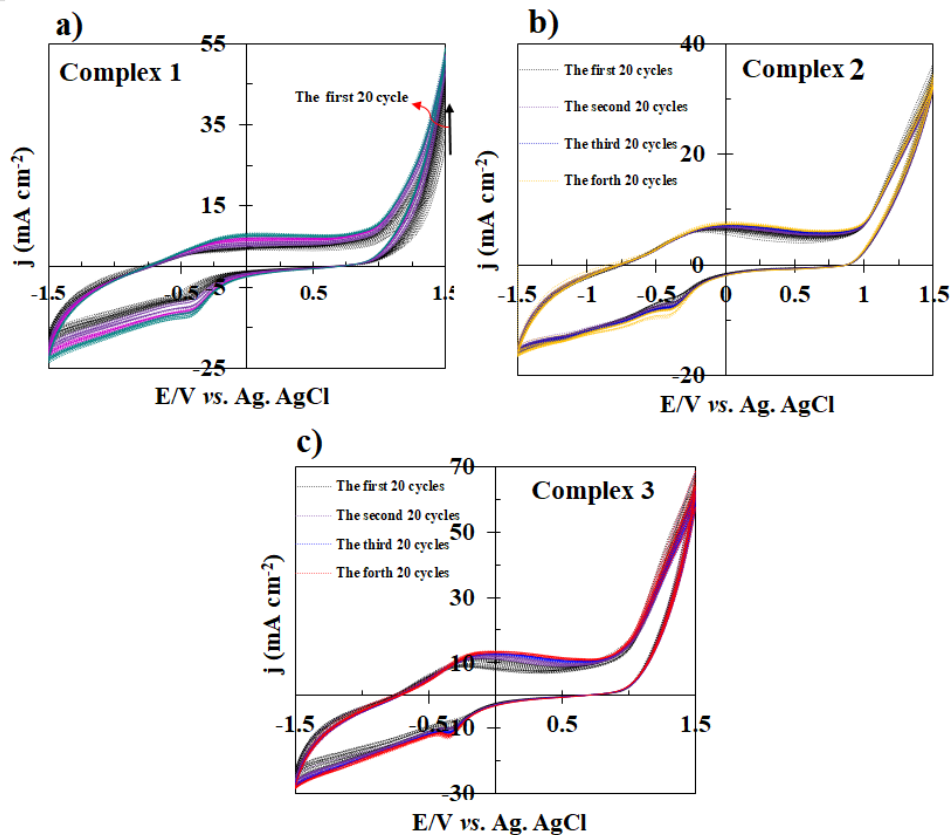


Figure 5: Continuous CVs for modified electrodes with Fe complexes 1-3 in borate buffer solution (25 ml, 0.5 M, and pH=11) at a scan rate of 50 mV s⁻¹.

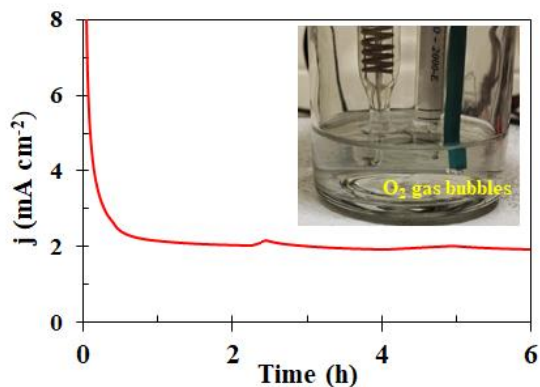


Figure 6: CA experiment for the modified electrode with complex 3 at a constant potential of 0.8 V for 6 h.

Conclusion

In the present research work, some new iron(III) complexes containing salophen ligands with different electron withdrawing substitutions (chlorine, bromine and nitro groups) were produced and characterized by conventional techniques. Then, the synthesized complexes were used as electrode materials and heterogeneous catalysts for electrochemical water oxidation in borate buffer solution. The results showed that all modified electrodes have high activity for the reaction compared to the unmodified electrode, and require relatively low overpotential to oxidize water in a constant current density. Complex **3** showed the best activity for water oxidation with overpotential values of 295 and 485 mV at j of 5 and 10 mA cm⁻². Calculations showed that the ECSA for complex **3** is higher than that of complexes **1** and **2**, indicating its higher active catalytic sites and improved water oxidation. This study showed that the Fe complexes with salophen ligands containing different substituents can be used as stable and molecular electrocatalysts for water oxidation.

Acknowledgment

The authors thank the financial support of Azarbaijan Shahid Madani University for this work.

References

[1] Back, D. F.; Oliveira, G. M.; Fontana, L. A.; Ramão, B. F.; Roman, D.; AlmeidaIglesias, B. J. *Mol. Struct.* 2015, 1100, 264.

[2] Keskoğlu, E.; Gündüzalp, A. B.; Çete, S.; Hamrcu, F.; Erk, B. *Spectrochim. Acta, Part A.* 2008, 70, 634.

[3] Cappillino, P. J.; Miecznikowski, J. R.; Tyler, L. A.; Tarves, P. C.; McNally, J. S.; Lo, W.; Kasibhatla, B. S. T.; Krzyaniak, M. D.; McCracken, J.; Wang, F.; Armstrong, W. H.; Caradonna, J. P.; *Dalton Trans.* 2012, 41, 5662.

[4] Baecker, D.; Ma, B. N.; Sagasser, J.; Schultz, L.; Hörschläger, C.; Weinreich, M.; Steiner, L.; Kircher, B.; Gust, R.; *Dalton Trans.* 2020, 49, 6842.

[5] Guerreiro, J. F.; Gomes, M. A. G.B.; Pagliari, F.; Jansen, J.; Marafioti, M. G.; Nistico, C.; Hanley, R.; Costa, R. O.; Ferreira, S. S.; Mendes, F.; Fernandes, C.; Horn, A.; Tirinato, L.; Seco, J.; *RSC Adv.* 2020, 10, 12699.

[6] Bouché, M.; Hognon, C.; Grandemange, S.; Monari, A.; Gros, P. C.; *Dalton Trans.* 2020, 49, 11451.

[7] Costas, M.; Mehn, M. P.; Jensen, M. P.; Jr, I. Q.; *Chem. Rev.* 2004, 104, 939.

[8] Corr, M. J.; Murphy, J. A.; *Chem. Soc. Rev.* 2011, 40, 2279.

[9] Kerns, S. A.; Rose, M.; *J. Acc. Chem. Res.* 2020, 53, 1637.

[10] Jastrzebski, R.; Weckhuysen, B. M.; Bruijninx, P. C. A.; *Chem. Commun.* 2013, 49, 6912.

[11] Shaw, S.; White, J. D. *Chem. Rev.* 2019, 119, 9381.

- [12] Bruijninx, P. C. A.; van Koten, G.; Klein Gebbink, R. J. M.; *Chem. Soc. Rev.* 2008, 37, 2716.
- [13] McQuilken, A. C.; Goldberg, D. P.; *Dalton Trans.* 2012, 41, 10883.
- [14] Crichton, R. R. *Biological inorganic chemistry: An Introduction*, Elsevier, Amsterdam, 2008.
- [15] Basak, T.; Das, D.; Ray, P. P.; Banerjee, S.; Chattopadhyay, S.; *CrystEngComm.* 2020, 22, 5170.
- [16] Rajnák, C.; Titiš, J.; Moncol, J.; Valigura, D.; Boča, R.; *Inorg. Chem.* 2020, 59, 14871.
- [17] Sharghi, H.; Aboonajmi, J.; Aberi, M.; *J. Org. Chem.* 2020, 85, 6567.
- [18] Çapan, A.; Uruş, S.; Sönmez, M.; *J. Saudi Chem. Soc.* 2018, 2022, 757.
- [19] Shaghaghi, Z.; Aligholivand, M.; Mohammad-Rezaei, R.; *Int. J. Hydrog. Energy.* 2021, 46, 389.
- [20] Aligholivand, M.; Shaghaghi, Z.; Bikas, R.; Kozakiewicz, A.; *RSC Adv.* 2019, 9, 40424.
- [21] Akhtar, M. N.; Bikas, R.; AlDamen, M, A.; Shaghaghi, Z.; Shahid, M.; Sokolov, A.; *Dalton Trans.* 2022, 51, 12686.
- [22] Shaghaghi, Z.; Kouhsangini, P.S.; Mohammad-Rezaei, R.; *Appl. Organomet. Chem.* 2021, 35, e6103.
- [23] Shaghaghi, Z.; Jafari, S.; Mohammad-Rezaei, R.; *J. Electroanal. Chem.* 2022, 915, 116369.
- [24] Kottrup, K. G.; Hetterscheid, D. G. H.; *Chem. Commun.* 2016, 52, 2643.
- [25] Acuña-Parés, F.; Costas, M.; Luis, J. M.; Lloret-Fillol, J.; *Inorg. Chem.* 2014, 53, 5474.
- [26] Hong, D.; Mandal, S.; Yamada, Y.; Lee, Y.-M.; Nam, W.; Llobet, A.; *Inorg. Chem.* 2013, 2, 9522.
- [27] Mukhopadhyay, S.; Basu, O.; Kar, A.; Das, S. K.; *Inorg. Chem.* 2020, 59, 472.
- [28] Panda, C.; Debgupta, J.; Díaz, D. D.; Singh, K. K.; Gupta, S. S.; Dhar, B. B.; *J. Am. Chem. Soc.* 2014, 136, 12273.
- [29] Coggins, M. K.; Zhang, M.-T.; Vannucci, A. K.; Dares, C. J.; Meyer, T. J.; *J. Am. Chem. Soc.* 2014, 136, 5531.
- [30] Praneeth, V. K. K.; Kondo, M.; Okamura, M.; Akai, T.; Izu, H.; Masaoka, S.; *Chem. Sci.* 2019, 10, 4628.
- [31] Mehrabani, S.; Bikas, R.; Zand, Z.; Mousazade, Y.; Allakhverdiev, S. I.; Najafpour, M. M.; *Int. J. Hydrog. Energy.* 2020, 45, 17434.
- [32] Shaghaghi, Z.; Bikas, R.; Tajdar, H., Kozakiewicz, A.; *J. Mol. Struct.* 2020, 1217, 128431.
- [33] Uysal, Ş.; Koç, Z. E.; *J. Mol. Struct.* 2018, 1165, 14.
- [34] Kocyigit, O.; Guler, E.; *J. Organomet. Chem.* 2011, 696, 3106.
- [35] Karatas, E.; Ucan, H. I.; *J. Heterocycl. Chem.* 2017, 54, 69.
- [36] Cakmak, D.; Bulut, T.; Uzun, D.; *Electroanalysis.* 2020, 32, 1559.
- [37] Shaghaghi, Z.; Kalantari, N.; Kheyrollahpoor, M.; Haeili, M.; *J. Mol. Struct.* 2020, 1200, 127107.
- [38] Shaghaghi, Z.; Mohammad-Rezaei, R.; Jafari, S.; *J. Electroanal. Chem.* 2022, 922, 116733.

- [39] Gruzdev, M. S.; Vorobeva, V. E.; Zueva, E. M.; Chervonova, U. V.; Petrova, M. M.; Domracheva, N. E.; Polyhedron. 2018, 155, 415.
- [40] Chervonova, U.V.; Gruzdev, M.S.; Zueva, E.M.; Vorobeva, V.E.; Ksenofontov, A. A.; Alexandrov, A. I.; Pashkova, T. V.; Kolker, A. M.; J. Mol. Struct. 2020, 1200, 127090.
- [41] Pramanik, H. A. R.; Paul, P.C.; Mondal, P.; Bhattacharjee, C. R.; J. Mol. Struct. 2015, 1100 496.
- [42] Kursunlu, A. N.; Guler, E.; Sevgi, F.; Ozkalp, B.; J. Mol. Struct. 2013, 1048, 476.
- [43] Bertha, O.; Park, S. M.; Bull. Korean. Chem. Soc. 2000, 21, 405.
- [44] Sabaté, F.; Gavara, R.; Giannicchi, I.; Bosque, R.; Dalla Cort, A.; Rodríguez, L.; New J. Chem, 2016, 40, 5714.
- [45] Akhtar, M. N.; AlDamen, M. A.; Bikas, R.; Shaghghi, Z.; Jafari, S.; Ibragimov A. B.; Int. J. Hydrog. Energy, 2024, 51, 383-394.